

2014

# A discrete crack propagation model for FRP-strengthened RC slabs

D Dias-da-Costa  
*University of Sydney*

G Ranzi  
*University of Sydney*

R Graca-e-Costa  
*University of Algarve*

Scott T. Smith  
*Southern Cross University, [scott.smith@scu.edu.au](mailto:scott.smith@scu.edu.au)*

---

## Publication details

Dias-da-Costa, D, Ranzi, G, Graca-e-Costa, R & Smith, ST 2015, 'A discrete crack propagation model for FRP-strengthened RC slabs', in ST Smith (ed.), *23rd Australasian Conference on the Mechanics of Structures and Materials (ACMSM23)*, vol. I, Byron Bay, NSW, 9-12 December, Southern Cross University, Lismore, NSW, pp. 415-420. ISBN: 9780994152008.

ePublications@SCU is an electronic repository administered by Southern Cross University Library. Its goal is to capture and preserve the intellectual output of Southern Cross University authors and researchers, and to increase visibility and impact through open access to researchers around the world. For further information please contact [epubs@scu.edu.au](mailto:epubs@scu.edu.au).

## A DISCRETE CRACK PROPAGATION MODEL FOR FRP-STRENGTHENED RC SLABS

**D. Dias-da-Costa\***

School of Civil Engineering, The University of Sydney  
Sydney, NSW 2006, Australia. [daniel.diasdacosta@sydney.edu.au](mailto:daniel.diasdacosta@sydney.edu.au) (Corresponding Author)

**G. Ranzi**

School of Civil Engineering, The University of Sydney  
Sydney, NSW, 2006, Australia. [gianluca.ranzi@sydney.edu.au](mailto:gianluca.ranzi@sydney.edu.au)

**R. Graça-e-Costa**

ICIST and CEPAC, University of Algarve, Portugal. [rcosta@ualg.pt](mailto:rcosta@ualg.pt)

**S.T. Smith**

School of Environment, Science and Engineering, Southern Cross University  
Lismore, NSW, 2480, Australia. [scott.smith@scu.edu.au](mailto:scott.smith@scu.edu.au)

### ABSTRACT

This manuscript presents a discrete crack approach enabling simulation of the progressive process of crack localisation and propagation, as well as its interaction with debonding of fibre-reinforced polymer (FRP) composites from concrete substrates. The numerical approach has been implemented with a non-iterative algorithm to efficiently overcome convergence difficulties produced by different sources of material non-linearity, such as concrete crushing and cracking, yielding of steel reinforcement and debonding of the FRP. The accuracy of the model has been validated against experimental results carried out on one-way simply-supported FRP-strengthened RC slabs, thus highlighting the ability of the proposed model to adequately capture the behaviour of the strengthened slab system.

### KEYWORDS

FRP, RC slabs, strengthening, discrete crack models, non-iterative algorithms.

### INTRODUCTION

Fibre-reinforced polymer (FRP) composites can be used for the strengthening of reinforced concrete (RC) members although the effectiveness of the FRP can be limited by debonding. Numerous studies to date have reported the FRP to debond at strains significantly below its rupture strain and this represents an under-utilisation of the strength and strain capacity of the FRP. Debonding is found to generally initiate at the base of flexural or flexural-shear cracks in an RC (flexural) member, or at the FRP plate end (Teng et al. 2003, Oehlers and Seracino 2004, Hollaway and Teng 2008). A real need therefore exists to understand and quantify the debonding phenomenon. While experiments are informative, they can become expensive and time consuming. Numerical simulations are therefore attractive although their development has lagged behind the extensive number of experimental investigations that have been reported to date. The development of numerical models is challenging since such models need to be capable of dealing with the interaction between cracking and flexure in



an RC member, with the FRP-to-concrete interface (Foster et al. 1996, Foster and Marti 2003, Pham and Al-Mahaidi 2007, Khomwan et al. 2010, Loo et al. 2012).

In this context, this manuscript presents the development of a numerical model based on the discrete crack approach. A non-iterative algorithm is applied to avoid convergence difficulties associated with the material non-linearity arising from concrete crushing and cracking, the yielding of steel reinforcement and debonding of the FRP. An energy criterion is applied which enables the load path to be identified, which in turn leads to the maximum dissipation of energy. In the following sections, the model is described in detail and validated against experimental results carried out on one-way simply supported FRP-strengthened RC slabs (Smith et al. 2011, 2013).

## IMPLEMENTATION

In-house finite element software is herein used which adopts embedded discontinuities to simulate discrete fracture in concrete. Microcracking is supposed to localise in a surface of discontinuity as soon as the tensile strength of the material is reached (Wells and Sluys 2001). Then, the crack progressively undergoes softening as damage progresses (Hillerborg et al. 1976) and it is assumed that the opening is transmitted to its neighbourhood by a rigid body motion (i.e. both translation and rotation). In this case, it can be shown that the variational principle governing the problem is:

$$\int_{\Omega \setminus \Gamma_d} (\nabla^s \delta \hat{\mathbf{u}}) : \boldsymbol{\sigma}(\boldsymbol{\varepsilon}) d\Omega = \int_{\Omega \setminus \Gamma_d} \delta \hat{\mathbf{u}} \cdot \mathbf{b} d\Omega + \int_{\Gamma_t} \delta \hat{\mathbf{u}} \cdot \mathbf{t} d\Gamma, \quad (1)$$

$$\int_{\Gamma_d} \delta \mathbf{u}^{+/-} \cdot \mathbf{t}^+ d\Gamma = \int_{\Omega^+} \delta \tilde{\mathbf{u}} \cdot \mathbf{b} d\Omega + \int_{\Gamma_t^+} \delta \tilde{\mathbf{u}} \cdot \mathbf{t} d\Gamma, \quad (2)$$

where  $\Omega$  is the body containing the discontinuity,  $\Gamma_d$ , and subjected to quasi-static body forces  $\mathbf{b}$  and stresses  $\mathbf{t}$  distributed over the external boundary  $\Gamma_t$ ;  $\boldsymbol{\sigma}$  is the stress tensor and  $\mathbf{t}^+$  is the stress across the crack;  $\mathbf{u}^{+/-}$  is the opening of the crack;  $\mathbf{u}$  is the total displacement field resulting from the regular displacement,  $\hat{\mathbf{u}}$ , and the displacement due to the opening of the discontinuities is  $\tilde{\mathbf{u}}$ .

The discretised equations at the element level can be directly derived from Eqs. (1) and (2) as:

$$\left[ \begin{array}{cc} \mathbf{K}_{\hat{\mathbf{a}}\hat{\mathbf{a}}}^e & -\mathbf{K}_{\hat{\mathbf{a}}\mathbf{w}}^e \\ -\mathbf{K}_{\mathbf{w}\hat{\mathbf{a}}}^e & \mathbf{K}_{\mathbf{w}\mathbf{w}}^e + \mathbf{K}_d^e + \mathbf{K}_p^e \end{array} \right] \left\{ \begin{array}{c} d\mathbf{a}^e \\ d\mathbf{w}^e \end{array} \right\} = \left\{ \begin{array}{c} d\hat{\mathbf{f}}^e \\ d\mathbf{f}_w^e - \left( \mathbf{H}_{\Gamma_d}^e \mathbf{M}_w^{ek} \right)^T d\hat{\mathbf{f}}^e \end{array} \right\}, \quad (3)$$

where  $\mathbf{a}^e$  are the nodal degrees of freedom associated with the total displacement;  $\mathbf{w}^e$  is the nodal opening of the discontinuity;  $\mathbf{K}_{\hat{\mathbf{a}}\hat{\mathbf{a}}}^e$  is the stiffness of a regular finite element;  $\mathbf{K}_d^e$  is the stiffness of the discontinuity;  $\mathbf{K}_{\hat{\mathbf{a}}\mathbf{w}}^e$ ,  $\mathbf{K}_{\mathbf{w}\hat{\mathbf{a}}}^e$  and  $\mathbf{K}_{\mathbf{w}\mathbf{w}}^e$  are matrices coupling the bulk element with the embedded discontinuity; and  $\hat{\mathbf{f}}^e$  and  $\mathbf{f}_w^e$  are, respectively, the regular nodal forces and the forces at the discontinuity, such that:  $\mathbf{K}_{\hat{\mathbf{a}}\mathbf{w}}^e = \mathbf{K}_{\hat{\mathbf{a}}\hat{\mathbf{a}}}^e \mathbf{H}_{\Gamma_d}^e \mathbf{M}_w^{ek}$ ,  $\mathbf{K}_{\mathbf{w}\hat{\mathbf{a}}}^e = \mathbf{K}_{\hat{\mathbf{a}}\mathbf{w}}^{eT}$ ,  $\mathbf{K}_{\mathbf{w}\mathbf{w}}^e = \left( \mathbf{H}_{\Gamma_d}^e \mathbf{M}_w^{ek} \right)^T \mathbf{K}_{\hat{\mathbf{a}}\hat{\mathbf{a}}}^e \mathbf{H}_{\Gamma_d}^e \mathbf{M}_w^{ek}$ ; and  $\mathbf{H}_{\Gamma_d}^e$  is a diagonal matrix containing ‘1’ in the degrees of freedom belonging to one side of the discontinuity, and ‘0’ otherwise. In the case where all forces are applied at the nodes,  $d\mathbf{f}_w^e - \left( \mathbf{H}_{\Gamma_d}^e \mathbf{M}_w^{ek} \right)^T d\hat{\mathbf{f}}^e = \mathbf{0}$ .

In Eq. (3),  $\mathbf{M}_w^{ek}$  is the matrix transmitting the opening of the discontinuity to the boundary nodes of the element, whereas  $\mathbf{K}_p^e$  is a penalty matrix enforcing constant shear jump along each discontinuity.

A detailed description of this procedure is provided by (Dias-da-Costa et al. 2010).

A discrete crack is introduced or propagated according to the Rankine criterion. For that purpose, the first principal stress is smoothed using an average support length of two or three times the typical

element size, as described in (Wells and Sluys 2001). Existing crack fronts are propagated from the crack tip and are oriented orthogonally to the first principle direction. In addition, new crack fronts are introduced at the centre of the bulk finite element whenever the first principal stress reaches the tensile strength. With regards to the implementation herein utilised, only one crack is allowed for each bulk element.

The resulting system of equations is solved using the Non-Iterative Energy Based Method (NIEM) (Graça-e-Costa et al. 2012, 2013), since it is capable of dealing with different sources of material non-linearity. For that purpose, an incremental analysis is performed until critical bifurcation points are found. Then, these points are overcome by switching to a total approach, where damage is prescribed according to the material behaviour observed before disregarding the wrong solution. At each step, an energy criterion allows selection of the path leading to the highest dissipation of energy (Gutiérrez 2004).

## VALIDATION

The numerical framework is validated using experimental results obtained on simply-supported one-way spanning RC slabs (Smith et al. 2011, 2013). A total of 4 slabs are considered herein. Two slabs represent the reference unstrengthened situations (i.e. specimens S1 and S2.1), while the two remaining slabs represent the FRP-strengthened specimens (i.e. S2 and S2.2).

The structural layout and the testing arrangement, with two line loads applied at 200 mm from mid-span, are shown in Fig. 1. The concrete for specimens S1 and S2 has a compressive cube strength of 51.7 MPa, a tensile strength of 3.3 MPa and a Young's modulus of 28.4 GPa. For specimens S2.1 and S2.2, the corresponding values are 39.9 MPa, 2.7 MPa and 26.9 GPa, respectively. The steel reinforcement consists of two 10 mm diameter bars as illustrated in Fig. 1b, with yield stress and Young's modulus of 566 MPa and 198 GPa, respectively. The unanchored but bonded FRP plate is formed by a wet lay-up procedure from three layers of carbon fibre sheet. The nominal thickness of each fibre sheet for specimen S2 is 0.166 mm, while the tensile strength at rupture and Young's modulus of the FRP are 3163 MPa and 239 GPa, respectively. For specimen S2.2, the nominal thickness of each fibre sheet, tensile strength at rupture and Young's modulus of the FRP are, respectively, 0.131 mm, 3644 MPa and 232 GPa.

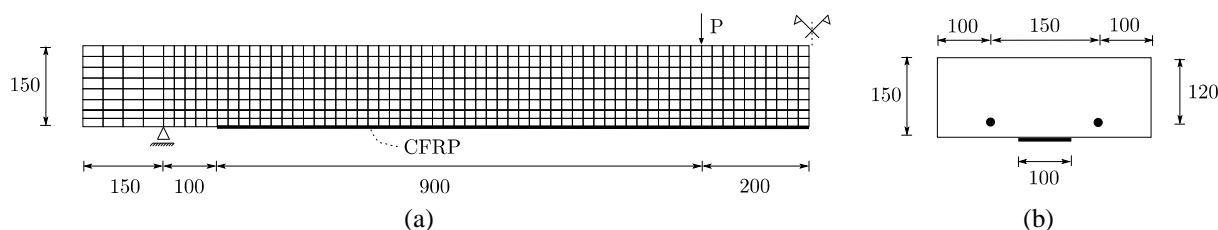


Figure 1. (a) Structural scheme and adopted finite element mesh; (b) cross-section.

The adopted finite element mesh is shown in Fig. 1a. Bilinear elements are used for the concrete with an elastic and perfect-plastic constitutive law under compression. In the case of tensile stresses, the bulk is linear elastic and the embedded discontinuity follows a bilinear softening traction-separation law. Both steel and FRP are modelled using truss elements, elastic and perfect plastic in the case of steel and linear elastic in the case of FRP. Standard interface elements are used to connect the steel and FRP elements to the concrete in order to simulate the bond behaviour. In the case of steel, the constitutive model proposed in Model Code 2010 is adopted (fib 2013), whereas the simplified model proposed by (Lu et al. 2005) is utilised for the FRP.

Fig. 2 compares both experimental and numerical results in terms of load versus displacement responses. It can be concluded that the model is capable of predicting the behaviour of both unstrengthened and strengthened specimens, as well as adequately identifying the initial stiffness, cracking load and tension-stiffening effect. In the case of strengthened specimens, a sudden load drop

is observed just after the peak load is reached. This is caused by the debonding of the FRP. After that, the structural response is identical to the one observed for the reference unstrengthened specimen. The schematic representation of the crack pattern is shown in Fig. 3 for slab S2.

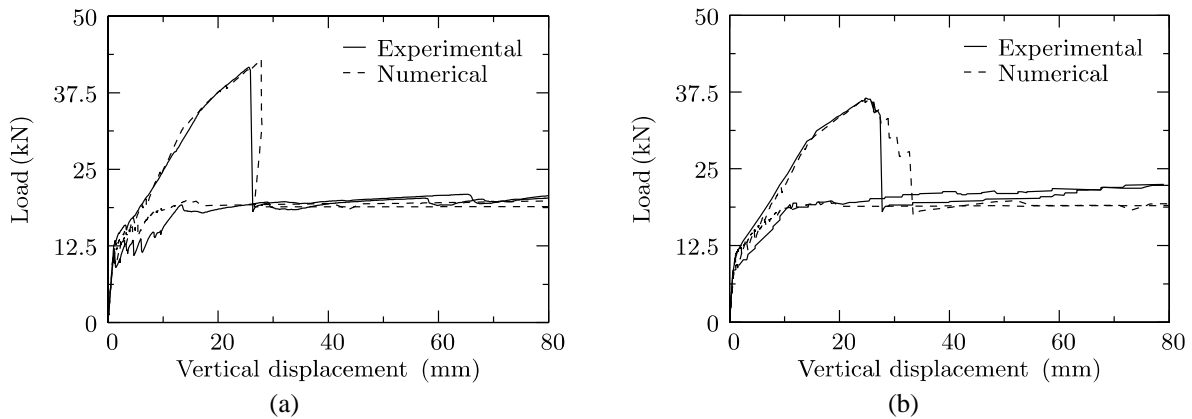


Figure 2. Load vs. displacement curves for specimens: (a) S1-S2; and (b) S2.1-S2.2

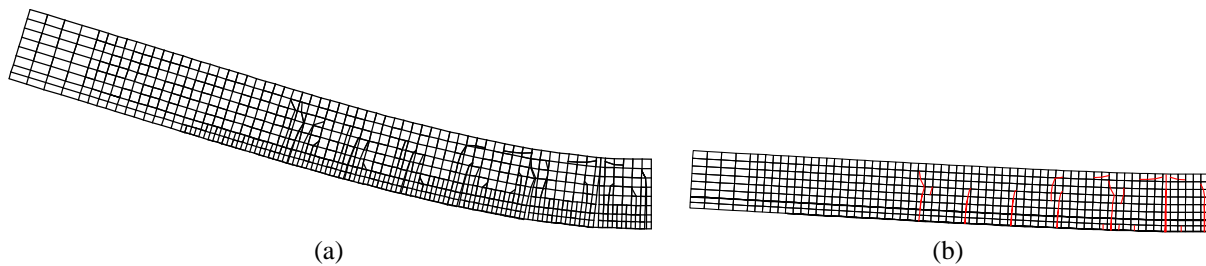


Figure 3. Crack pattern after the peak load for specimen S2: (a) representation of all embedded cracks (displacements magnified 10x); and (b) representation of active cracks (displacements magnified 2x).

## PARAMETRIC STUDY

This section presents a brief parametric study on the performance of FRP-strengthened slabs that highlights the influence of the number of layers of carbon fibres sheet, as well as the bond length on the overall structural response. The comparisons have been carried out using the numerical model previously developed for specimen S2 as reference (i.e. with three layers of 2200 mm FRP, see Fig. 1a) and varying the FRP arrangements as discussed in the following sub-sections.

### Number of FRP Layers

Different strengthening layers of FRP have been considered and these have been varied between one to four layers of carbon fibre sheet. The corresponding load versus displacement curves are shown in Fig. 4a.

The obtained results highlight that by increasing the number of layers, the maximum load increases almost linearly (see Fig. 4b). Conversely, the displacement at the maximum load of the structure decreases significantly, as can be observed in Fig. 4a.

### Bond Length

The bond between the FRP plate and concrete substrate is a critical element in the behaviour of the strengthened member. To identify how this parameter changes the structural behaviour, different bond lengths are considered, ranging from 1040 to 2200 mm. Fig. 5 shows the structural response for all models.

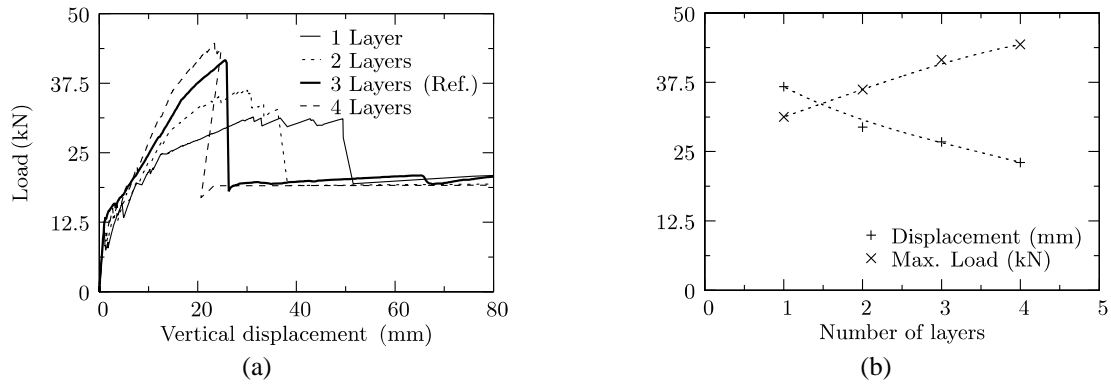


Figure 4. Number of layers of CFRP: (a) Load vs. displacement; and (b) peak load and corresponding displacement vs. number of layers.

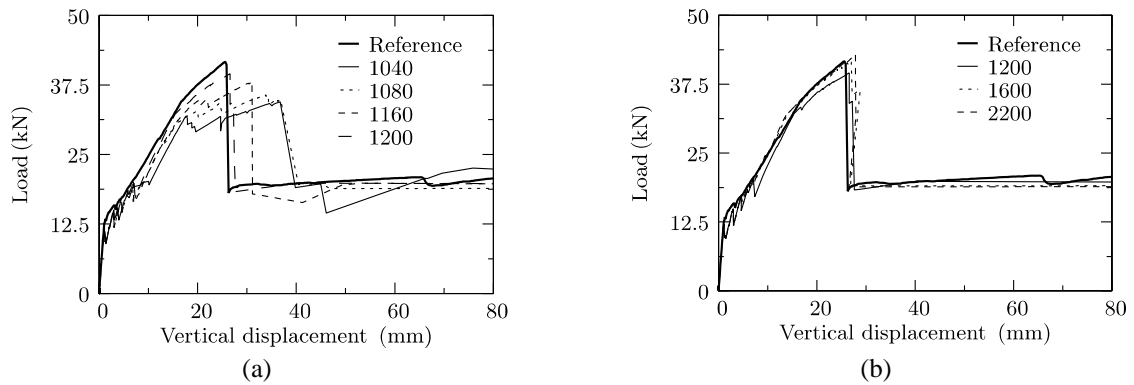


Figure 5. Bond length: (a) shorter anchorage length; (b) longer anchorage length.

Figs. 5 and 6 highlight that an increase in strength is exhibited by the strengthened slab with FRP sheets up to a length of about 1600 mm (i.e. 2/3 of the clear span). After this length, no additional strength benefit is observed. This represents an optimum retrofitting strategy for strength.

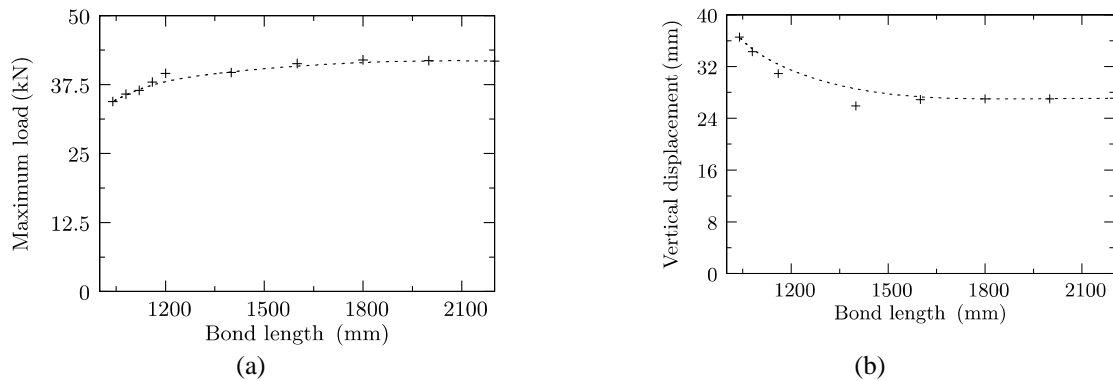


Figure 6. (a) Maximum load vs. bond length; (b) vertical displacement at peak load vs. bond length.

## CONCLUSIONS

This manuscript has presented a computational approach for the simulation of the behaviour of FRP-strengthened slabs. This approach was developed using a discrete crack approach with the finite element formulation relying on embedded discontinuities in the simulation of fracture propagation and localisation in concrete elements. The adopted non-iterative solution-finding algorithm NIEM provided an adequate representation of the structural response, effectively avoiding the usual convergence difficulties found with classic iterative procedures.

Comparison with experimental results has shown that the model is capable of predicting the overall structural response, including the development of cracks, tension-stiffening effects and the sudden loss of load carrying capacity produced by the debonding process. A brief parametric study was carried out to illustrate the sensitivity of the strengthened slab for different FRP arrangements.

## ACKNOWLEDGEMENTS

This work was supported by Australian Research Council's Discovery Projects funding scheme (project number DP140100529) and by FEDER through the Operational Programme for Competitiveness Factors – COMPETE – and through FCT (project number FCOMP-01-0124-FEDER-020275 / FCT ref. PTDC/ECM/119214/2010).

## REFERENCES

- Dias-da-Costa, D., Alfaiate, J., Sluys, L.J. and Júlio, E.N.B.S. (2010) "A comparative study on the modelling of discontinuous fracture by means of enriched nodal and element techniques and interface elements", *International Journal of Fracture*, Vol. 161, No. 1, pp. 97-119.
- fib (2013). *Model Code for Concrete Structures 2010*, Wiley-VCH Verlag GmbH & Co. KGaA.
- Foster, S. and Marti, P. (2003) "Cracked Membrane Model: Finite Element Implementation", *Journal of Structural Engineering*, Vol. 129, No. 9, pp. 1155-1163.
- Foster, S.J., Budiono, B. and Gilbert, R.I. (1996) "Rotating crack finite element model for reinforced concrete structures", *Computers & Structures*, Vol. 58, No. 1, pp. 43-50.
- Graça-e-Costa, R., Alfaiate, J., Dias-da-Costa, D., Neto, P. and Sluys, L.J. (2013) "Generalisation of non-iterative methods for the modelling of structures under non-proportional loading." *International Journal of Fracture*, Vol. 182, No. 1, pp. 21-38.
- Graça-e-Costa, R., Alfaiate, J., Dias-da-Costa, D. and Sluys, L.J. (2012) "A non-iterative approach for the modelling of quasi-brittle materials", *International Journal of Fracture*, Vol. 178, No. 1-2, pp. 281-298.
- Gutiérrez, M.A. (2004) "Energy release control for numerical simulations of failure in quasi-brittle solids", *Communications in Numerical Methods in Engineering*, Vol. 20, No. 1, pp. 19-29.
- Hillerborg, A., Modeer, M. and Petersson, P.E. (1976) "Analysis of crack formation and crack growth in concrete by means of fracture mechanics and finite elements", *Cement and Concrete Research*, Vol. 6, No. 6, pp. 773-781.
- Hollaway, L.C. and Teng, J.G. (2008) *Strengthening and rehabilitation of civil infrastructures using fibre-reinforced polymer (FRP) composites*. Cambridge (UK), Woodhead Publishing Limited.
- Khomwan, N., Foster, S.J. and Smith, S.T. (2010) "FE Modeling of FRP-Repaired Planar Concrete Elements Subjected to Monotonic and Cyclic Loading", *Journal of Composites for Construction*, Vol. 14, No. 6, pp. 720-729.
- Loo, K., Foster, S.J. and Smith, S.T. (2012) "FE Modeling of CFRP-Repaired RC Beams Subjected to Fatigue Loading", *Journal of Composites for Construction*, Vol. 16, No. 5, pp. 572-580.
- Lu, X.Z., Teng, J.G., Ye, L.P. and Jiang, J.J. (2005) "Bond-slip models for FRP sheets/plates bonded to concrete", *Engineering Structures*, Vol. 27, No. 6, pp. 920-937.
- Oehlers, D.J. and Seracino, R. (2004) *Design of FRP and steel plated RC structures: retrofitting beams and slabs for strength, stiffness and ductility*. UK, Elsevier.
- Pham, H.B. and Al-Mahaidi, R. (2007) "Modelling of CFRP-concrete shear-lap tests", *Construction and Building Materials*, Vol. 21, No. 4, pp. 727-735.
- Smith, S.T., Hu, S., Kim, S.J. and Seracino, R. (2011) "FRP-strengthened RC slabs anchored with FRP anchors", *Engineering Structures*, Vol. 33, No. 4, pp. 1075-1087.
- Smith, S.T., Zhang, H.W. and Wang, Z. (2013) "Influence of FRP anchors on the strength and ductility of FRP-strengthened RC slabs", *Construction and Building Mat.*, Vol. 49, pp. 998-1012.
- Teng, J.G., Smith, S.T., Yao, J. and Chen, J.F. (2003) "Intermediate crack-induced debonding in RC beams and slabs." *Construction and Building Materials*, Vol. 17, No. 6-7, pp. 447-462.
- Wells, G.N. and Sluys, L.J. (2001) "A new method for modelling cohesive cracks using finite elements", *International Journal for Numerical Methods in Engineering*, Vol. 50, No. 12, pp. 2667-2682.